ACS APPLIED MATERIALS & INTERFACES

Research Article

www.acsami.org

Multifunctional Properties of Cyanate Ester Composites with SiO_2 Coated Fe_3O_4 Fillers

Weixing Sun,[†] Wuzhu Sun,[‡] Michael R. Kessler,[†] Nicola Bowler,[†] Kevin W. Dennis,[§] R. William McCallum,[§] Qi Li,*[,‡] and Xiaoli Tan*[,†]

[†]Department of Materials Science and Engineering, Iowa State University, Ames, Iowa 50011, United States

[‡]Institute of Metal Research, Chinese Academy of Sciences, 72 Wenhua Road, Shenyang, 110016, P. R. China

[§]Division of Materials Science and Engineering, Ames Laboratory, U.S.-DOE, Ames, Iowa 50011, United States

ABSTRACT: SiO_2 coated Fe_3O_4 submicrometer spherical particles (a conducting core/insulating shell configuration) are fabricated using a hydrothermal method and are loaded at 10 and 20 vol % into a bisphenol E cyanate ester matrix for synthesis of multifunctional composites. The dielectric constant of the resulting composites is found to be enhanced over a wide frequency and temperature range while the low dielectric loss tangent of the neat cyanate ester polymer is largely preserved up to 160 °C due to the insulating SiO_2 coating on individual conductive Fe_3O_4 submicrometer spheres. These composites also demonstrate high dielectric breakdown strengths at room temperature. Dynamic mechanical analysis indicates that the storage modulus of the composite with a 20 vol % filler loading is twice as high as that of neat resin, but the glass transition temperature considerably decreases with increasing filler content. Magnetic measurements reveal a large saturation magnetization and negligibly low coercivity and remanent magnetization in these composites.

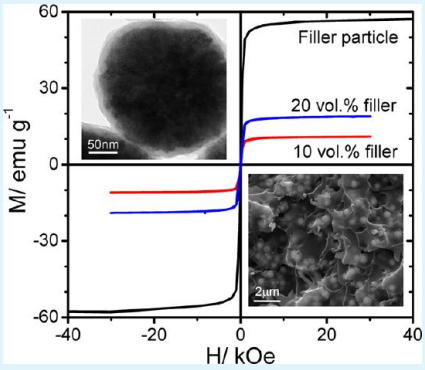

KEYWORDS: *SiO_2 coated Fe_3O_4 submicrometer spheres, polymer−matrix composites, dielectric properties, mechanical stiffening, superparamagnetic behavior*

INTRODUCTION

In recent years, weight reduction of aerospace vehicles has become critically important for improved efficiency and reduced operating costs.[1,2] Aerospace structures typically consist of multiple systems each performing diverse functions with corresponding subcomponents. Significant weight savings may be achieved, however, using materials that simultaneously perform multiple functions. These so-called multifunctional materials provide an approach for increased efficiency by integrating functions such as energy storage, or sensing, into structural materials. Polymer−matrix composites (PMCs), which have been widely used for aerospace structures because of their outstanding specific strength and specific stiffness, lend themselves naturally to the concept of multifunctionality. Because of the way that PMCs are processed, it is convenient to incorporate various kinds of fillers into polymer matrixes to perform multiple functions for overall system weight reduction.

Structural capacitors are multifunctional devices that store electrical energy while simultaneously carrying mechanical loads.[3] For the capacitor function, both conductive and ferroelectric ceramic fillers have been studied to improve the dielectric constant in PMCs. The incorporation of a large amount of conductive fillers such as metal particles and carbon nanotubes, however, also brings a high dielectric loss, adversely affecting energy storage.[4−6] It should be noted that, in studies of the dielectric properties of PMCs with ferroelectric ceramic particle fillers, the mechanical properties are usually not reported.[7−9] There is a need for extensive research on processing and characterization of multifunctional PMCs for the development of structural capacitors.

Additional functional properties of PMCs, e.g., magnetic properties, may lead to further weight reduction when they are employed in multifunctional parts and devices. Electrically conductive Fe_3O_4, in either bulk or nanoscale form, has been widely used for magnetic recording, bioimaging, magnetic bioseparation, and microwave absorption thanks to its excellent magnetic properties.[10−12] Furthermore, Fe_3O_4 particles with different coatings have been shown to display a variety of new features compared to their bulk counterpart.[13,14] Therefore, Fe_3O_4 nanoparticles with special coatings, when used as fillers in PMCs, are expected to impart unique functional properties to the composites.

In the present work, Fe_3O_4 submicrometer sized spheres (~0.4 μm in diameter) composed of nanoscale grains (~10−20 nm in size) were coated with a thin electrically insulating SiO_2 layer (~10 nm). When incorporated into a polymer matrix, the conductive Fe_3O_4 core is anticipated to improve the dielectric constant while the insulating SiO_2 shell will confine the charge

Received: October 30, 2012
Accepted: February 11, 2013
Published: February 22, 2013

transport and keep the dielectric loss low. In addition, the high Young's modulus of Fe_3O_4 will stiffen the composite very effectively.[15] Of course, the excellent magnetic properties of Fe_3O_4 particles will make the composites magnetically responsive. Bisphenol E cyanate ester (BECy) is chosen as the polymer matrix for its excellent mechanical performance and high thermal stability (an onset T_g of 280 °C was reported for neat BECy).[16,17] Additionally, the BECy monomer shows an extremely low viscosity in the range of 0.09 to 0.12 Pa s at room temperature,[18] which is extremely helpful for processing composites with good filler dispersion.

EXPERIMENTAL SECTION

Synthesis of SiO_2 Coated Fe_3O_4 Submicrometer Spheres. A hydrothermal method was employed to synthesize the core−shell structured Fe_3O_4−SiO_2 spheres. For the Fe_3O_4 core fabrication,[19] $FeCl_3{\cdot}6H_2O$ (2.7 g, Sinopharm Chemical Reagent Corporation, P.R. China) was dissolved in ethylene glycol (80 mL, Sinopharm Chemical Reagent Corporation) to form a clear solution. Sodium acetate (7.2 g, Sinopharm Chemical Reagent Corporation) and polyethylene glycol (2.0 g, Sinopharm Chemical Reagent Corporation) were then added into the clear solution. The mixture was stirred vigorously for 30 min and subsequently sealed in an autoclave. The autoclave was then heated to 180 °C and held for 10 h. With the assistance of alkali produced by sodium acetate, Fe^{3+} ions underwent hydrolysis and were partially reduced by ethylene glycol to form Fe_3O_4 primary nanograins. To minimize the surface energy, these primary nanograins gradually aggregated into large spherical particles. Sodium acetate also served as the electrostatic stabilizer in the synthesis, and polyethylene glycol served as the surfactant. Thus, further aggregation of the large spherical particles was prevented, and the quasi-monodispersed Fe_3O_4 spheres were formed. After it was cooled down to room temperature (25 °C), black powder of Fe_3O_4 was collected. The powder was washed several times with ethanol and dried at 40 °C for 12 h.

The Stöber method[20] was employed to coat the as-produced Fe_3O_4 spherical particles with a SiO_2 layer. In this process, 0.1 g of Fe_3O_4 powder was washed with 0.1 M HCl (Beijing Chemical Corporation, P.R. China) solution and dispersed in a mixture of ethanol (80 mL, Beijing YiLi Fine Chemical Corporation, P.R. China) and deionized water (20 mL,18.25 MΩ) by ultrasonication for 10 min. Then, 1 mL of ammonia solution (25%, Sinopharm Chemical Reagent Corporation) and 0.1 mL of tetraethyl orthosilicate (TEOS, Tianjin Kermel Chemical Reagents Development Center, P.R. China) were added into the solution quickly under continuous mechanical stirring. After 6 h of stirring at room temperature, the product was collected by a magnet. The powder was washed repeatedly with a water/ethanol mixture (50w/50w) and dried at 40 °C for 12 h.

Processing of BECy−Matrix Composites. SiO_2 coated Fe_3O_4 submicrometer spheres were dried at 200 °C for 10 h to eliminate absorbed moisture in order to prevent a chemical reaction between water molecules and BECy monomers during curing.[21] The BECy monomers (TenCate Advanced Composites, USA) were mixed with an organometallic-based polymerization catalyst supplied by the manufacturer in a ratio of 100:3. The mixture was incorporated with the dried SiO_2 coated Fe_3O_4 spheres, then sonicated, and mixed at 1−2 min intervals with a sonic dismembrator (Model 100, Fisher Scientific, USA). The mixture was further processed in a planetary mixer (Mazerustar KK50S, KURABO Industries Ltd., Japan) for approximately 30 min to remove possible air bubbles and to improve particle dispersion. The slurry was then injected into two stainless steel molds using a 10 mL syringe. The molds were moved into a rotational oven to cure the polymer for 2 h at 150 °C and another 2 h at 250 °C. Two batches of composites were fabricated with 32 and 51 wt % SiO_2 coated Fe_3O_4 particles. Taking the average volume fraction of the SiO_2 layer into consideration, this corresponds to 10 and 20 vol % filler loadings of the composite. For each batch, two disk-shaped samples with diameters of 11 and 22 mm were fabricated for subsequent dielectric and mechanical tests, respectively.

Characterization of the SiO_2 Coated Fe_3O_4 Submicrometer Spheres and the Composites. Prior to SiO_2 coating, the as-processed Fe_3O_4 spheres were analyzed with powder X-ray diffraction (D/MAX-2004, Rigaku Corporation, Japan) for phase purity. The morphology of these spherical particles was examined with scanning electron microscopy (SEM, SUPRA35, ZEISS, Germany) as well as transmission electron microscopy (TEM, JEOL 2010, JEOL, Japan). X-ray photoelectron spectroscopy (XPS) measurements on the as-processed Fe_3O_4 and SiO_2 coated Fe_3O_4 submicrometer spheres were conducted using an ESCALAB250 X-ray Photoelectron Spectrometer (Thermo Fisher Scientific Inc., Waltham, MA, U.S.A.) with an Al K anode (1486.6 eV photon energy, 300 W). The microstructure of SiO_2 coated Fe_3O_4 spheres was also analyzed with TEM to determine the thickness of the SiO_2 layer. Fourier transform infrared spectroscopy (FTIR, Bruker IFS66 V, with resolution of 2 cm^{-1}) was used to measure the infrared spectrum of SiO_2 coated Fe_3O_4 spheres. The magnetic properties of the SiO_2 coated Fe_3O_4 submicrometer spheres were measured with a Magnetic Property Measurement System (Quantum Design, Inc., USA).

Fracture surfaces of composite samples with 10 and 20 vol % filler loadings were observed with SEM (Quanta FEG 250, FEI, USA) to examine the particle dispersion in the polymer matrix. Dielectric properties of composites and neat BECy were characterized with a Novocontrol dielectric spectrometer (Novocontrol Technologies, Germany) in a frequency range from 1 Hz to 1 MHz at a series of temperatures up to 200 °C. Dielectric breakdown strength of the composites was evaluated by a CEAST Dielectric Rigidity Instrument (Instron, USA) at a voltage ramp rate of 0.5 kV s^{-1} and a current intensity of 10 mA. Thermomechanical analysis (TMA) of composite samples was carried out with a Q400 DMA instrument (TA Instruments, USA), and dynamic mechanical analysis (DMA) was conducted using a Q800 model DMA instrument (TA Instruments, USA) at a heating rate of 3 °C/min. Magnetic hysteresis loops of the composites were recorded with a Magnetic Property Measurement System (Quantum Design, Inc., USA) at room temperature.

RESULTS AND DISCUSSION

Microstructure and Magnetic Properties of the Fe_3O_4 Submicrometer Spheres. X-ray diffraction was performed on the black Fe_3O_4 powder prior to SiO_2 coating. The spectrum displayed in Figure 1 can be indexed with a single spinel phase, indicating that the product is pure Fe_3O_4. Both SEM and TEM examinations indicate the particles are spherical with a quasi-uniform size. The diameter is determined to be 400 ± 100 nm. Figure 2a shows a representative TEM micrograph for these Fe_3O_4 spherical particles. These particles display a complex

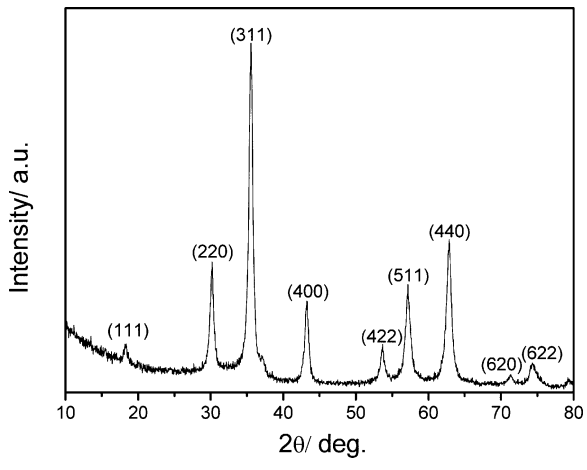

Figure 1. X-ray diffraction spectrum of Fe_3O_4 submicrometer spheres prior to SiO_2 coating.

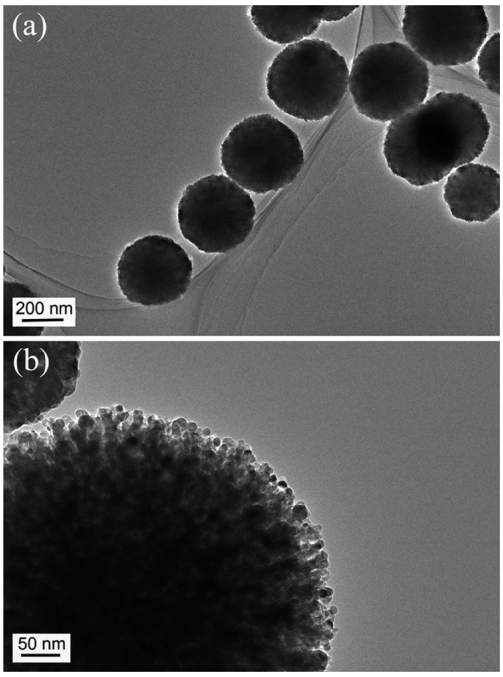

Figure 2. TEM micrographs of Fe_3O_4 submicrometer spheres prior to SiO_2 coating.

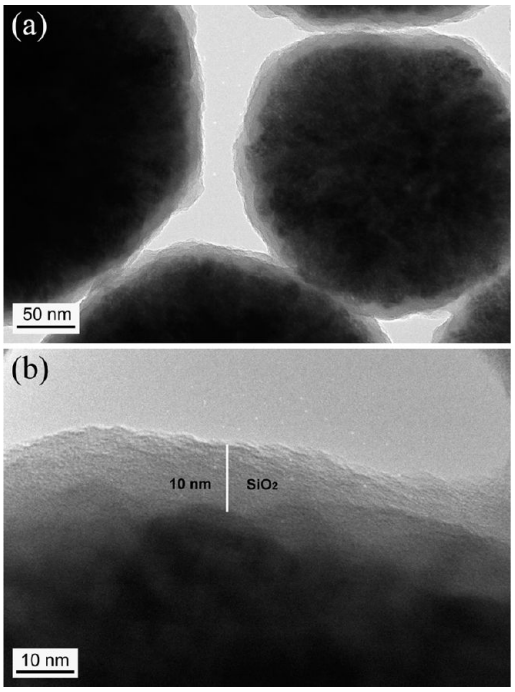

Figure 3. TEM micrographs of Fe_3O_4–SiO_2 core–shell submicrometer spheres.

microstructure; each sphere is composed of aggregated fine grains with sizes from 10 to 20 nm (Figure 2b). The observed fine grain size is consistent with the crystallite size estimated from their X-ray diffraction analysis. The surface region seems to be rough and highly porous, which is beneficial to the adhesion of the SiO_2 layer in the following synthesis step. Such hierarchical fine structure is believed to be critical to the resulting dielectric and magnetic properties in the composites.

The voids in the surface region of these Fe_3O_4 spheres are completely filled by the subsequent SiO_2 coating, as revealed by TEM examination (Figure 3). The Fe_3O_4/SiO_2 composite particles show a typical core–shell structure with a dense and continuous shell of amorphous SiO_2. The SiO_2 coating layer is uniform with a thickness about 10 nm. This value corresponds to a 93 vol % (96 wt %) of Fe_3O_4 in the Fe_3O_4/SiO_2 composite particles.

In addition to TEM, the presence of the SiO_2 surface layer was also verified by XPS analysis. Figure 4a shows the representative XPS survey spectra of the Fe_3O_4 submicrometer spheres prior to and after SiO_2 coating. The contrast is clear. The Fe 2p peak was detected only in Fe_3O_4 spheres prior to SiO_2 coating while the Si 2s and 2p peaks are seen in those submicrometer spheres after SiO_2 coating. The presence of the C 1s peak in both XPS spectra is due to the ambient environment. Figure 4b demonstrates the FTIR spectrum of SiO_2 coated Fe_3O_4 spheres. It reveals strong hydroxyl stretching (3434 cm^{-1}) and bending (1629 cm^{-1}) vibrations of physically adsorbed H_2O[22] and the stretching vibrations (943 cm^{-1}) of hydroxyl groups on oxides (Si–OH).[23] The result indicates that SiO_2 coated Fe_3O_4 spheres have high adsorption capacities to H_2O and hydroxyl groups exist on their surfaces.

The magnetization vs magnetic field hysteresis loop of the SiO_2 coated Fe_3O_4 spheres was recorded at room temperature and is shown in Figure 5. The saturation magnetization, M_S, is ~60 emu g^{-1}. This value is slightly lower than the bulk value[24] but consistent with previous reports on Fe_3O_4 nano-

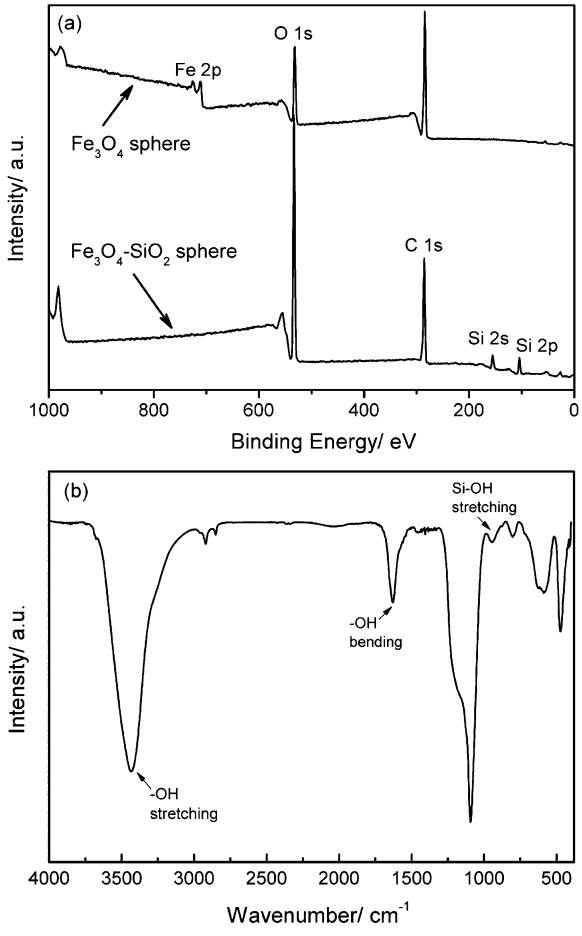

Figure 4. (a) Representative XPS survey spectra of the Fe_3O_4 spheres prior to and after SiO_2 coating; (b) the FTIR spectrum of SiO_2 coated Fe_3O_4 spheres.

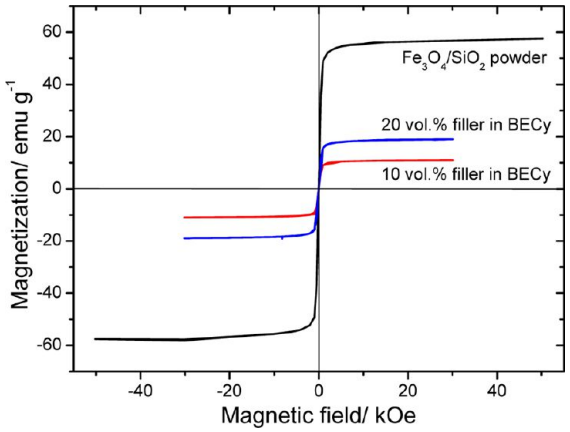

Figure 5. Magnetization vs magnetic field relations for Fe_3O_4/SiO_2 composite submicrometer spheres measured at room temperature. The data for the BECy–matrix composites are also displayed and are discussed in the Magnetic Properties of the BECy–Matrix Composites section.

particles.[25,26] However, the coercive field, H_C, and the remanent magnetization, M_R, of these submicrometer spheres are nearly zero, which indicates typical superparamagnetic behavior.[27,28] The demonstrated superparamagnetism in the spheres is attributed to the fine grain size (~10 to 20 nm), which is lower than the critical size (~30 nm) for superparamagnetism in Fe_3O_4.[29] Thus, these SiO_2 coated Fe_3O_4 spherical particles display no magnetization without external magnetic fields but demonstrate a strong magnetic response when an external magnetic field is present.

Microstructure of the BECy–Matrix Composites. SEM observations were conducted to investigate the filler dispersion in the polymer matrix. Figure 6 shows micrographs of fracture

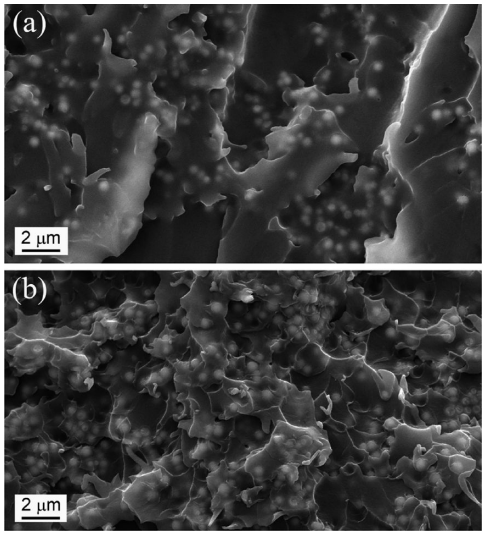

Figure 6. SEM micrographs of fracture surfaces of the BECy–matrix composites with (a) 10 vol % and (b) 20 vol % filler loadings.

surfaces of BECy–matrix composites with 10 and 20 vol % loadings of Fe_3O_4–SiO_2 core–shell spheres. Very few fine air bubbles (in dark contrast with size less than 1 μm) can be seen. Most importantly, it is observed that these submicrometer spheres are relatively well dispersed in the BECy matrix in composites with both loadings. The filler dispersion is attributed to the multiple mixing steps and the use of a rotating oven in the curing process. In addition, it appears that fracture primarily occurs within the BECy polymer matrix, indicating strong interfacial bonding at the particle/polymer interface. The good dispersion and the strong interface are likely the reason for the high dielectric breakdown strength in both composites, which will be elaborated in detail later.

Dielectric Properties of the BECy–Matrix Composites. Dielectric properties of the BECy–matrix composites were studied over a wide frequency and temperature range, as shown in Figures 7 and 8. Figure 7a reveals that the dielectric constant

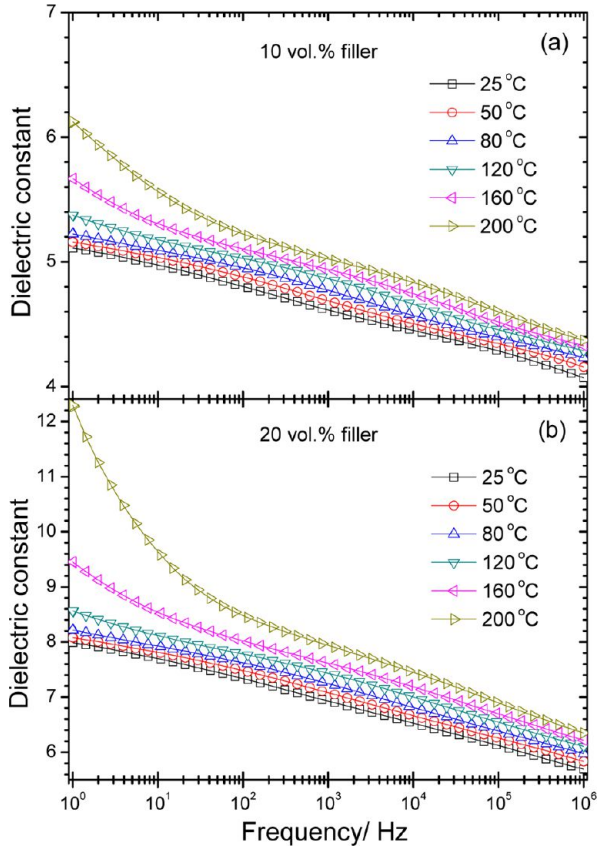

Figure 7. Frequency dependence of the dielectric constant at a series of temperatures in the BECy–matrix composites with 10 vol % (a) and 20 vol % (b) filler loadings.

of the BECy–matrix composite with 10 vol % particle loading is 5.1 at 1 Hz at room temperature, an increase of 1.7 times the dielectric constant of the neat BECy (3.0).[30] Similarly, at 20 vol % particle loading (Figure 7b), the dielectric constant is further improved to 8.0 at 1 Hz at room temperature, approximately 2.6 times that of neat BECy. It is noted that, while neat BECy shows an almost frequency-independent dielectric constant,[30] the BECy–matrix composite with 10 vol % particle loading displays a dielectric constant in the range of 4.1 to 5.1 within the measured frequency range. The frequency dependence of the dielectric constant gets stronger in the BECy–matrix composite with 20 vol % particle loading.

The loss tangent of the BECy–matrix composites increases with increasing filler content and also increases with measuring frequency. As shown in Figure 8, the maximum values of the loss tangent at room temperature are found to be 3.5% and 4.9% for composites with 10 and 20 vol % particle loadings,

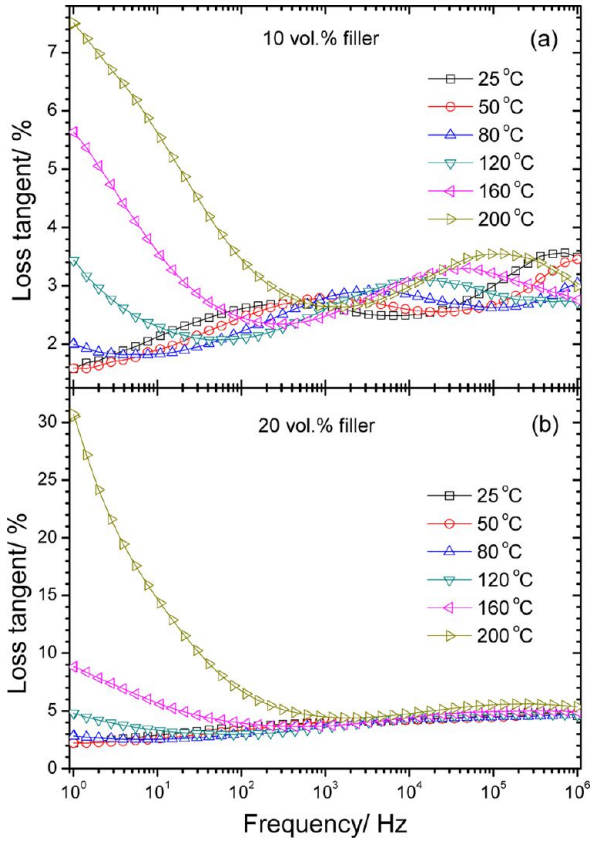

Figure 8. Frequency dependence of the loss tangent at a series of temperatures in the BECy–matrix composites with 10 vol % (a) and 20 vol % (b) filler loadings.

respectively, in the frequency range of 1 Hz to 1 MHz. Compared to our previously studied BECy–matrix composites reinforced with SiO_2 coated Si nanoparticles,[30] the composites in the present study show a slightly higher loss tangent. However, compared to other composites with conductive fillers,[31] the BECy–matrix composites with SiO_2 coated Fe_3O_4 spheres display a much suppressed loss tangent, especially at low frequencies. The SiO_2 shell confines the charge carrier motion within the Fe_3O_4 core, pushing the percolation threshold to a higher volume fraction. It should be pointed out that the grain boundary layer between very fine grains in the Fe_3O_4 core may also have played a role in suppressing the loss tangent of the BECy–matrix composites.

In order to explore potential applications as dielectrics in electrical capacitors, these BECy–matrix composites were investigated for their dielectric properties at various temperatures up to 200 °C, as also shown in Figures 7 and 8. Figure 7 exhibits dielectric constant of composites as a function of temperature. As shown in Figure 7a, the dielectric constant shows a gradual increase with rising temperatures in the whole frequency range for the composite filled with 10 vol % Fe_3O_4/SiO_2 spherical fillers. The relatively weak frequency dependence of the dielectric constant at room temperature is preserved at temperatures up to 120 °C. The increase in dielectric constant at 160 and 200 °C is accelerated in the frequency range of 1 to 100 Hz. Similar temperature dependence is shown in Figure 7b for the composite with 20 vol % filler loading, and the rapid increase of dielectric constant with respect to frequency decrease is more significant due to the higher conductive filler loading. It is significant to note in Figure 8a that, when the temperature is below 160 °C, the loss tangent remains under 3.5% at all frequencies. However, the loss tangent in this composite increases sharply as frequency decreases from 100 to 1 Hz at 160 and 200 °C, reaching maximum values of 5.6% and 7.5%, respectively. Figure 8b shows that the maximum loss tangent for the composite with 20 vol % filler loading reaches 8.8% at 160 °C and exceeds 10.0% when the frequency is below 30 Hz at 200 °C. Due to the high loss, this composite may not be a good candidate for dielectrics to be used at 200 °C and low frequencies. The high dielectric loss at low frequencies at elevated temperatures is attributed to the electrical conduction of the fillers. However, it is clear from Figure 8b that the composite with 20 vol % particle loading still demonstrates excellent dielectric performances for frequencies above 1 kHz at temperatures up to 200 °C. Therefore, the results indicate that the BECy–matrix composites with SiO_2 coated Fe_3O_4 submicrometer spheres are promising candidates for capacitor applications over a wide temperature and frequency range.

The dielectric breakdown strength (E_{br}) of these composites was measured at room temperature. E_{br} of composites with 10 and 20 vol % fillers are 29 and 26 MV/m, respectively, while that of neat BECy is 30 MV/m. In sharp contrast to the BECy–matrix composites reinforced with SiO_2 coated Si nanoparticles,[30] the composites in the present study do not show a large decrease in the dielectric breakdown strength. This is probably due to the homogeneous dispersion of the SiO_2 coated Fe_3O_4 particles and the strong particle/matrix interface (see Figure 6). The high dielectric breakdown strength of the neat BECy polymer is well preserved in the composite even with a 20 vol % filler loading. Taking the dielectric constant at 1 Hz at room temperature in this composite, for example, and assuming it is independent of applied electric field, the maximum electrical energy storage density of the BECy–matrix composite with 20 vol % filler loading is 0.024 J cm^{-3}. This value is two times that of neat BECy.

Thermomechanical Properties of the BECy–Matrix Composites. For potential structural capacitor applications, the thermomechanical properties of the composites need to be evaluated. TMA measurements indicate a linear thermal expansion coefficient of 47.2 and 37.7 ppm/°C around room temperature for the BECy–matrix composites with 10 and 20 vol % filler loading, respectively. Compared with the value of neat BECy (56.5 ppm/°C),[32] incorporating SiO_2 coated Fe_3O_4 particles suppresses the thermal expansion. This can be attributed to the low thermal expansion coefficient of these ceramic fillers. Figure 9 displays the storage modulus (E') and mechanical tan δ of the BECy–matrix composites as a function of temperature measured with a dynamic mechanical analyzer. The neat BECy data are also included for comparison. As shown in Figure 9a, E' is increased by factors of 1.7 and 2.4 at 40 °C from that of neat BECy by incorporating 10 and 20 vol % SiO_2 coated Fe_3O_4 particles, respectively. The composite with 20 vol % particle loading displays a storage modulus of 5.8 GPa at 40 °C. Compared to the Si/BECy nanocomposites,[30] SiO_2 coated Fe_3O_4 particles are more effective in stiffening the polymer matrix, thanks to the higher Young's modulus of Fe_3O_4.

The onset glass transition temperature (onset T_g) can be determined as the temperature at which E' exhibits a steep decrease, and it is slightly lower than the peak value of mechanical tan δ in Figure 9b. While neat BECy presents a remarkably high onset T_g among thermoset polymers at 280 °C, the incorporation of SiO_2 coated Fe_3O_4 fillers adversely

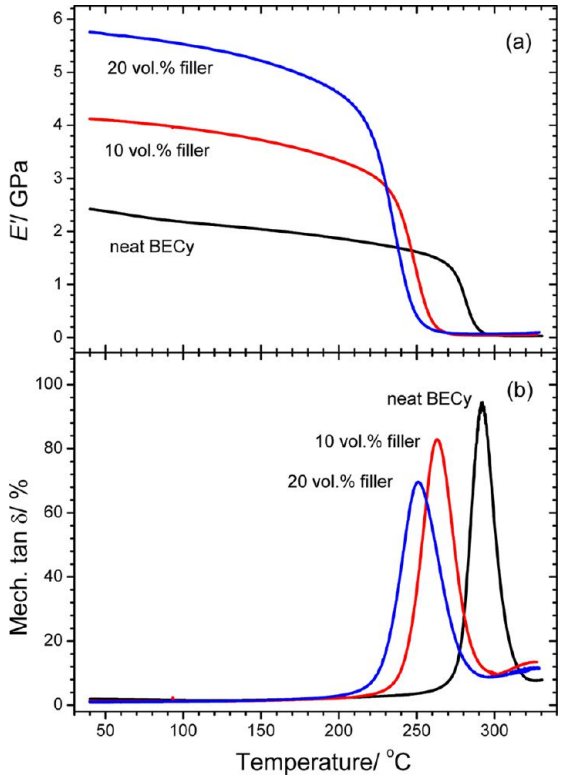

Figure 9. Storage modulus (E') (a) and mechanical tan δ (b) of the BECy–matrix composites and the neat BECy polymer as a function of temperature.

diminishes the T_g. The onset T_g is measured to be 246 and 230 °C for the composites filled with 10 and 20 vol % particles. This T_g suppression is consistent with results from other studies with bisphenol E cyanate ester, which showed similar reductions in glass transition relaxation when incorporating barium titanate,[21] nanoscale silica,[33] and nanoscale alumina.[34] Rather than being caused by incomplete cure of the resin, this decrease in T_g may be the result of changes to the network structure that develops in the presence of the active hydroxyl groups on the nanoparticles' surfaces (see FTIR results shown in Figure 4) during network formation. However, the results confirm that these composites are good candidate dielectrics for structural capacitors but only at temperatures below ca. 200 °C.

Magnetic Properties of the BECy–Matrix Composites. The SiO_2 coated Fe_3O_4 submicrometer spheres exhibit superparamagnetism with a strong saturation magnetization (Figure 5). Incorporating these magnetic particles into the BECy matrix imparts magnetic properties to the resulting composites, as shown in Figure 5. The magnetization developed under 30 kOe is measured to be 11 and 19 emu g^{-1} for the BECy–matrix composites with 10 and 20 vol % filler loading, respectively. These values are lower than those estimated from the sphere mass fractions in the composites, and the discrepancy may be due to residual oil-based coolant from the cutting of the small pieces with a low speed diamond saw for magnetic measurements. Inherited from the SiO_2 coated Fe_3O_4 fillers, the BECy–matrix composites display superparamagnetic behavior. As a result, these BECy–matrix composites will respond to the presence of external magnetic fields and could have a magnetic sensing capability.

CONCLUSIONS

In summary, SiO_2 coated Fe_3O_4 submicrometer spheres with a quasi-uniform size were successfully fabricated. These particles develop strong magnetization under applied magnetic fields and appear to be superparamagnetic. When incorporated into the BECy polymer, the SiO_2 coated Fe_3O_4 fillers bring multiple functional properties to the Fe_3O_4/SiO_2/BECy three phase composites. The dielectric constant of the composites is significantly enhanced because of the conductive Fe_3O_4 core, while the dielectric loss is still low because of the insulating SiO_2 shell. Most importantly, the dielectric breakdown strength only slightly decreases. As a result, the electrical energy storage capability is doubled in the composite with 20 vol % filler loading compared to the neat polymer. Additionally, the storage modulus of the composites is greatly increased compared to that of neat BECy, indicating a significant stiffening effect of the SiO_2 coated Fe_3O_4 particles. Furthermore, high saturation magnetizations are observed in these composites. Therefore, the BECy–matrix composites reinforced with SiO_2 coated Fe_3O_4 fillers are promising for multifunctional devices which may lead to significant weight reductions and efficiency enhancement over conventional composites and monofunctional components.

AUTHOR INFORMATION

Corresponding Author

*E-mail: qili@imr.ac.cn (Q.L.); xtan@iastate.edu (X.T.).

Notes

The authors declare no competing financial interest.

ACKNOWLEDGMENTS

This work was supported by NASA (Cooperative Agreement No. NNX09AP70A), the Knowledge Innovation Program of the Institute of Metal Research (Grant No. Y0N5A111A1), and the Youth Innovation Promotion Association, Chinese Academy of Sciences (Grant No. Y2N5711171).

ABBREVIATIONS

PMC = polymer–matrix composite
BECy = bisphenol E cyanate ester

REFERENCES

(1) Burton, R. L.; Brown, K.; Jacobi, A. M. *J. Spacecr. Rockets* **2006**, *43*, 696–698.
(2) Koelle, D. E. *Acta Astronaut.* **2003**, *53*, 797–803.
(3) Curtis, P. T. *Adv. Perform. Mater.* **1996**, *3*, 279–293.
(4) Zhou, T.; Zha, J.; Hou, Y.; Wang, D.; Zhao, J.; Dang, Z. *ACS Appl. Mater. Interfaces* **2011**, *3*, 4557–4560.
(5) Xu, J.; Moon, K. S.; Tison, C.; Wong, C. P. *IEEE Trans. Adv. Packag.* **2006**, *29*, 295–306.
(6) Li, C.; Thostenson, E. T.; Chou, T. W. *Compos. Sci. Technol.* **2008**, *68*, 1227–1249.
(7) Stefanescu, E. A.; Tan, X.; Lin, Z.; Bowler, N.; Kessler, M. R. *Polymer* **2010**, *51*, 5823–5832.
(8) Stefanescu, E. A.; Tan, X.; Lin, Z.; Bowler, N.; Kessler, M. R. *Polymer* **2011**, *52*, 2016–2024.
(9) Wang, G. *ACS Appl. Mater. Interfaces* **2010**, *2*, 1290–1293.
(10) Bate, G. In *Ferromagnetic materials*; Wohlfahrt, E. P., Eds.; North Holland Publ. Co.: Amsterdam, Netherlands, 1986.
(11) Sen, T.; Sebastianelli, A.; Bruce, I. J. *J. Am. Chem. Soc.* **2006**, *128*, 7130–7131.
(12) Pardoe, H.; Chua-anusorn, W.; St. Pierre, T. G.; Dobson, J. *J. Magn. Magn. Mater.* **2001**, *225*, 41–46.

(13) Mukhopadhyay, A.; Joshi, N.; Chattopadhyay, K.; De, G. *ACS Appl. Mater. Interfaces* **2012**, *4*, 142−149.
(14) Chen, W.; Yi, P.; Zhang, Y.; Zhang, L.; Deng, Z.; Zhang, Z. *ACS Appl. Mater. Interfaces* **2011**, *3*, 4085−4091.
(15) Wang, Q.; Yang, F.; Yang, Q.; Chen, J.; Guan, H. *Mater. Des.* **2010**, *31*, 1023−1028.
(16) Hamerton, I.; Hay, J. N. *High Perform. Polym.* **1998**, *10*, 163−174.
(17) Sheng, X.; Akinc, M.; Kessler, M. R. *Mater. Sci. Eng., A* **2010**, *527*, 5892−5899.
(18) Shimp, D. A.; Craig, W. M., Jr. *Proc. 34th Int. SAMPE Symp.* **1989**, *34*, 1336−1346.
(19) Deng, H.; Li, X.; Peng, Q.; Wang, X.; Chen, J.; Li, Y. *Angew. Chem., Int. Ed.* **2005**, *44*, 2782−2785.
(20) Stöber, W.; Fink, A.; Bohn, E. *J. Colloid Interface Sci.* **1968**, *26*, 62−69.
(21) Chao, F.; Bowler, N.; Tan, X.; Liang, G.; Kessler, M. R. *Compos., Part A: Appl. Sci.* **2009**, *40*, 1266−1271.
(22) Zhdanov, S. P.; Kosheleva, L. S.; Titova, T. I. *Langmuir* **1987**, *3*, 960−967.
(23) Chaudhary, Y. S.; Ghatak, J.; Bhatta, U. M.; Khushalani, D. *J. Mater. Chem.* **2006**, *16*, 3619−3623.
(24) Ni, S.; Lin, S.; Pan, Q.; Yang, F.; Huang, K.; He, D. *J. Phys. D: Appl. Phys.* **2009**, *42*, 055004-1−055004-5.
(25) Wang, X.; Li, W.; Luo, L.; Fang, Z.; Zhang, J.; Zhu, Y. *J. Appl. Polym. Sci.* **2012**, *125*, 2711−2715.
(26) Barbeta, V. B.; Jardim, R. F.; Kiyohara, P. K.; Effenberger, F. B.; Rossi, L. M. *J. Appl. Phys.* **2010**, *107*, 073913.
(27) Maity, D.; Kale, S. N.; Kaul-Ghanekar, R.; Xue, J. M.; Ding, J. *J. Magn. Magn. Mater.* **2009**, *321*, 3093−3098.
(28) Xiao, L.; Li, J.; Brougham, D. F.; Fox, E. K.; Feliu, N.; Bushmelev, A.; Schmidt, A.; Mertens, N.; Kiessling, F.; Valldor, M.; Fadeel, B.; Mathur, S. *ACS Nano* **2011**, *5*, 6315−6324.
(29) Yang, T.; Brown, R.; Kempel, L.; Kofinas, P. *J. Magn. Magn. Mater.* **2008**, *320*, 2714.
(30) Sun, W.; De León, J. E.; Ma, C.; Tan, X.; Kessler, M. R. *Compos. Sci. Technol.* **2012**, *72*, 1692−1696.
(31) Lu, J.; Moon, K.; Xu, J.; Wong, C. P. *J. Mater. Chem.* **2006**, *16*, 1543−1548.
(32) Badrinarayanan, P.; Kessler, M. R. *Compos. Sci. Technol.* **2011**, *71*, 1385−1391.
(33) Goertzen, W. K.; Kessler, M. R. *Compos., Part A: Appl. Sci.* **2008**, *39*, 761−768.
(34) Sheng, X.; Akinc, M.; Kessler, M. R. *Polym. Eng. Sci.* **2010**, *50*, 302−311.